Kobe J. Med. Sci., Vol. 67, No. 2, pp. E61-E70, 2021

Protective Effects of Endothelin-2 Expressed in Epithelial Cells on Bleomycin-Induced Pulmonary Fibrosis in Mice

ARISTI INTAN SORAYA[1,2], YOKO SUZUKI[1], MITSURU MORIMOTO[3], CHEMYONG JAY KO[4], KOJI IKEDA[5], KEN-ICHI HIRATA[2], and NORIAKI EMOTO[1,2] *

[1]*Laboratory of Clinical Pharmaceutical Science, Kobe Pharmaceutical University, 4-19-1 Motoyamakita, Higashinada, Kobe, 658-8558, Japan*

[2]*Division of Cardiovascular Medicine, Department of Internal Medicine, Kobe University Graduate School of Medicine, 7-5-1 Kusunoki, Chuo, Kobe, 650-0017, Japan*

[3]*Laboratory for Lung Development and Regeneration, RIKEN Center for Biosystems Dynamics Research, Kobe 650-0047, Japan*

[4]*Department of Comparative Biosciences, College of Veterinary Medicine, University of Illinois at Urbana-Champaign, 2001 South Lincoln Avenue, Urbana, IL 61802, USA.*

[5]*Department of Epidemiology for Longevity and Regional Health, Kyoto Prefectural University of Medicine, 465 Kajii, Kawaramachi-Hirokoji, Kamigyou, Kyoto 6028566, Japan*

** Corresponding author*

Received 16 July 2021/ Accepted 5 August 2021

Keywords: endothelin-2, epithelial cells, pulmonary fibrosis, fibroblast

Initially, endothelin (ET)-2 was described as an endothelium-derived vasoconstrictor. However, accumulating evidence suggests the involvement of ET-2 in non-cardiovascular physiology and disease pathophysiology. The deficiency of ET-2 in mice can be lethal, and such mice exhibit a distinct developmental abnormality in the lungs. Nonetheless, the definite role of ET-2 in the lungs remains unclear. The ET-2 isoform, ET-1, promotes pulmonary fibrosis in mice. Although endothelin receptor antagonists (ERAs) show improvements in bleomycin-induced pulmonary fibrosis in mouse models, clinical trials examining ERAs for pulmonary fibrosis treatment have been unsuccessful, even showing harmful effects in patients. We hypothesized that ET-2, which activates the same receptor as ET-1, plays a distinct role in pulmonary fibrosis. In this study, we showed that ET-2 is expressed in the lung epithelium, and *ET-2* deletion in epithelial cells of mice results in the exacerbation of bleomycin-induced pulmonary fibrosis. *ET-2* knockdown in lung epithelial cell lines resulted in increased apoptosis mediated via oxidative stress induction. In contrast to the effects of ET-1, which induced fibroblast activation, ET-2 hampered fibroblast activation in primary mouse lung fibroblast cells by inhibiting the TGF-β–SMAD2/3 pathway. Our results demonstrated the divergent roles of ET-1 and ET-2 in pulmonary fibrosis pathophysiology and suggested that ET-2, expressed in epithelial cells, exerts protective effects against the development of pulmonary fibrosis in mice.

INTRODUCTION

Endothelins (ETs) are a family of 21 amino acid peptides comprising three isoforms (ET-1, ET-2, and ET-3) that activate the canonical G protein-coupled receptors (GPCRs), endothelin A (ET_A) and endothelin B (ET_B) receptors (1). ET-3 is unique because it differs from other peptides by six amino acids and has a low binding affinity to ET_A (2). ET-2, previously characterized as a vasoactive intestine contractor in rodents (3), and ET-1 exhibit a similar structure with only two different amino acids and a similar binding affinity to ET_A and ET_B. ET-2 and ET-1 peptides released from endothelial cells demonstrate the same vasoconstrictive potency in all isolated human vessels (2). As ET-1 expression is more abundant in cells, ET-2 is often assumed to mimic ET-1. Hence, previous studies mainly focused on ET-1 rather than ET-2 (4).

ET-2 plays a distinct role in ovarian physiology (5) and retinal angiogenesis (6). It is involved in mediating the functions of the immune (7) and gastrointestinal systems (8) as well as the pathophysiology of several diseases, such as heart failure (9) and cancers (10,11). In addition, ET-2 is regulated by numerous transcription factors, including epidermal growth factor, TNF-α, hypoxia-inducible factor 1-alpha, forskolin, and pituitary gonadotropins (12). Notably, global ET-2 knockout in mice is lethal to the animals owing to abnormal lung development (13). This observation demonstrates the crucial role of ET-2 in lung physiology.

ET-1 expression is upregulated in patients with pulmonary fibrosis (14). ET-1 transgenic mice develop progressive pulmonary fibrosis (15), demonstrating the role of ET-1 in this disease. Furthermore, bleomycin-induced lung fibrosis in mice showed improvement after treatment with an endothelin receptor

Phone: +81-78-441-7536 Fax: +81-78-441-7536 E-mail: emoto@kobepharma-u.ac.jp

antagonist (ERA) (16), suggesting that blocking the ET-1 pathway could be a viable strategy to manage lung fibrosis. However, clinical trials targeting ET-1 with ERA have shown disappointing results in idiopathic pulmonary fibrosis and systemic sclerosis-induced interstitial lung disease (17–19). These conflicting evidences suggest that the ET-2 peptide, which acts on the same receptors, has a different role from ET-1 in the pathophysiology of pulmonary fibrosis.

We hypothesized that ET-2 may have protective effects against the pathophysiology of pulmonary fibrosis, in contrast to ET-1. To test this hypothesis, we investigated the effect of ET-2 deletion in epithelial cells on bleomycin-induced pulmonary fibrosis using ET-$2^{flox/flox}$; SHH-$Cre^{+/-}$ mice. Furthermore, we utilized the lung epithelial cell line and isolated lung fibroblast as in vitro study to explore the distinct role of ET-2 and ET-1 in lung fibrosis pathophysiology. Our findings may provide a novel insight about the involvement of ET-2 in pulmonary fibrosis pathophysiology and contribute to the future development of its therapeutic approach.

MATERIALS AND METHODS

Antibodies

Antibody for RFP (#ab124754) and pro-SFTPC (#ab211326) were purchased from Abcam (Cambridge, UK). Anti-αSMA (#F3777) was purchased from Sigma-Aldrich (St. Louis, MO). Antibody for cleaved-caspase-3 (#9661s), caspase-3 (#9662s), caspase-8 (#9746), caspase-9 (#9508), phospho-SMAD2/3 (#8828s), SMAD2/3 (#3102s), phospho-AMPKα (#2535), and GAPDH (#2118s) were purchased from Cell Signaling Technology (Beverly, MA). Donkey anti-Rabbit IgG Alexa488 (#A-21206) or Alexa549 (#A-21207) for immunofluorescence analysis were obtained from Thermo Fisher Scientific (Waltham, MA). Horseradish peroxidase-conjugated goat anti-rabbit IgG (#7074s) or anti-mouse IgG (#7076s) for immunoblot analysis were obtained from Cell Signaling Technology.

Animal studies

The development of ET-2-iCre, ET-2-iCre; ROSA26-lacZ, and ET-2-iCre; Ai9 mouse lines (12) and ET-$2^{flox/flox}$ mouse line (6) has been described previously. We crossed ET-$2^{flox/flox}$ mice with SHH-Cre mice (20) to generate an epithelial-specific *ET-2* knockout, ET-$2^{flox/flox}$; SHH-$Cre^{+/-}$ mice. The mice were maintained with a 12-h light-dark cycle and fed a standard chow diet (CRF-1, Charles River Laboratories International, Wilmington, MA). Littermate ET-$2^{flox/flox}$ mice were used as controls. All experimental animal protocols were approved by the Ethics Review Committee for Animal Experiments of Kobe Pharmaceutical University.

Histological analysis

The lungs were inflated and fixed in 4% paraformaldehyde (Wako Pure Chemical, Osaka, Japan) for 24 h, followed by paraffin embedding. 4 μm lung tissue sections were stained using X-Gal, Hematoxylin-Eosin, Masson's trichrome, or immunofluorescence staining, and observed under Keyence BZ-8100 fluorescence microscope (Keyence Corp, Osaka, Japan). The fibrotic and αSMA-positive areas were measured using ImageJ (National Institute of Health, https://imagej.nih.gov/ij/).

Gene expression analysis

RNA was isolated using RNAiso Plus (TAKARA, Tokyo, Japan) and purified using NucleoSpin RNA Purification (Macherey-Nagel, Düren, Germany). cDNA was synthesized using PrimeScript RT Reagent Kit with gDNA Eraser (TAKARA). PCR was performed using FastStart SYBR Green Master (Roche Applied Science, Basel, Switzerland) followed by quantitative PCR analysis using LightCycler96 (Roche Applied Science) for selected primers (Table I).

Lung mechanics

The mice were anesthetized with 2,2,2-Tribromoethanol (Sigma-Aldrich), tracheostomized, paralyzed with 30 μg of Pancuronium bromide (Sigma-Aldrich), and connected to a computer-controlled ventilator (flexiVent, SCIREQ, Quebec, Canada). Lung mechanic parameters were then measured by flexiWare. Each maneuver was repeated until at least two acceptable measurements were recorded, and the mean of the measurements was calculated.

Induction of pulmonary fibrosis

The protocol was performed as described previously, with minor modifications (21). 11-12 weeks old mice were anesthetized with isoflurane (Pfizer, NY) inhalation via Meratec (Senko Medical Instrument, Tokyo, Japan), and a midline cervical incision was made to expose the trachea. A 22-gauge cannula was inserted into the trachea to administer 5 mg/kg of bleomycin (Lexsy Bleo, Jena Bioscience, Jena, Germany) in 60 μL of sterile 0.9%

normal saline (vehicle). Sham control mice were administered the vehicle. The mice were briefly connected to a small animal ventilator unit (Muromachi Kikai, Tokyo, Japan) before closing the subcutaneous fascia and skin incision.

Cell culture

A549 cells were cultured in RPMI medium (Sigma-Aldrich) supplemented with 10% fetal bovine serum (FBS, Gibco, Waltham, MA) and 1% penicillin/streptomycin (PS, Sigma-Aldrich). siRNA-mediated silencing of *ET-1* (siGENOME SMARTpool Human *ET-1*, M-016692-02-0005, Dharmacon, Lafayette, CO), *ET-2* (CCAGGUGGAGGAAGAGAUAUU, Dharmacon), or silencer negative control siRNA (Thermo Fisher Scientific) were administered using Lipofectamine RNAiMax (Thermo Fisher Scientific). Apoptosis was induced by incubating cells with serum-free RPMI for 24 h before adding 500 μM H_2O_2 (Wako Pure Chemical) for 6 h. In some experiments, the cells were treated with 300 μM H_2O_2 for the indicated duration or stained with 2 μM dihydroethidium (Calbiochem, San Diego, CA).

Determination of ET-1/ET-2 levels in the lung tissue and cell media

Frozen lung samples were weighed and homogenized (Polytron, Elkhart, IND) in a 10× buffer containing 4% acetic acid and protease inhibitor cocktail (Sigma-Aldrich) on ice. Homogenates were immediately placed in boiling water for 10 min, cooled in ice for another 10 min, and centrifuged at 15,000 rpm at 4°C for 30 min. The supernatant was collected, applied to Sep-Pak C-18 plus (Waters, Milford, MA), and eluted with 4% acetic acid and 86% ethanol solution. The eluates were evaporated using a centrifugal evaporator (EYELA, Tokyo Rikakikai, Tokyo, Japan) and resuspended in QuantiGlo ET-1 immunoassay assay buffer (R&D Systems) (22). Cell medium samples were analyzed by direct application of the same immunoassay according to the manufacturer's instructions.

Production of cell lysates and immunoblotting

The cells were lysed in radioimmunoprecipitation assay (RIPA) buffer containing phosphatase and protease inhibitor cocktail (Sigma-Aldrich) and centrifuged for 15 min at 15,000 rpm. Protein content was measured with a detergent compatible (DC) Assay (Bio-Rad, Hercules, CA). The proteins were separated using SDS–polyacrylamide gels and then transferred onto nitrocellulose membranes (Bio-Rad). The membranes were blocked with 5% skim milk (Wako Pure Chemical) in Tris-buffered saline-Tween for 30 min at 23-25°C. Immunoblots were probed with a primary antibody at 4°C for 16 h, followed by incubating with a secondary antibody for 60 min at room temperature. For cleaved-caspase-3 detection, we used Can Get Signal Immunoreaction Enhancer Solution (Toyobo, Osaka, Japan) for antibody dilution. After brief incubation with Clarity Western ECL substrate (Bio-Rad) or Amersham ECL Select (GE, Boston, MA), bands were detected using ChemiDoc (Bio-Rad).

Fibroblast isolation

The protocol was performed as described previously, with additional modifications (23). Lung tissues from C57BL/6J mice were minced and digested five times for 10 min each at 37°C in digestion buffer. The digestion buffer was prepared using 1 mg/mL collagenase IV (Gibco), 100 μg/mL deoxyribonuclease I (Roche Applied Science), and 1 mg/mL bovine serum albumin pH 7 (Sigma-Aldrich) in Hanks' Balanced Salt Solution supplemented with Ca^{2+} and Mg^{2+} (Gibco) then passed through a 0.2 μm filter (Advantec Toyo Kaisha, Tokyo, Japan). The digested tissue was then filtered through a 100 μm cell strainer (Falcon, Corning, NY), centrifuged at 1,500 rpm for 10 min, washed with Ack Lysing Buffer (Gibco), and cultured in low-glucose DMEM (Sigma-Aldrich) supplemented with 10% FBS and 1% PS. The experiments were performed at passage three.

The lung fibroblast medium was replaced with a serum-free medium for 24 h, and the cells were incubated with 100 nM recombinant ET-1 or ET-2 (#4198 or #4209, Peptide Institute) for 1 h. The cells were then treated with 10 ng/mL TGF-β1 (#240-B, R&D System, Minneapolis, MN) for 1 h or 24 h.

Migration assay

$4x10^4$ mouse lung fibroblasts in 300 μL serum-free medium were loaded into the top chamber of a modified Boyden chamber (Falcon). 100 nM recombinant ET-1, ET-2 peptide or vehicle in 500 μL serum-free medium was loaded into the bottom chamber. After incubation for 6 h at 37°C with 5% CO_2, the cells were fixed, stained with Mayer's hematoxylin (Wako Pure Chemical), and counted under microscope.

Statistical analysis

Statistical analyses were performed using GraphPad Prism software version 8 (GraphPad Software, San Diego, CA). All data are presented as mean ± SEM and analyzed using Student's two-tailed t-test or 1-way

ANOVA followed by Tukey post hoc test. Statistical significance was set at $p < 0.05$.

RESULTS

ET-2 is expressed in mouse lung epithelial cells

To identify the cells that express ET-2 in the lungs, we utilized a previously described transgenic mouse line (12) expressing codon-improved Cre recombinase (iCre) driven by the *ET-2* gene promoter and β-galactosidase under a universal promoter, termed ET-2-iCre; ROSA26-lacZ mice. We found that X-Gal-stained ET-2 recombination was localized in the respiratory epithelium and alveolar pneumocytes **(Fig. 1A)**. To further confirm the cells expressing ET-2, we used ET-2-iCre; Ai9 mice that exhibited red fluorescence protein (RFP) in cells with functional iCre expression. RFP-marked ET-2 recombination was observed in the bronchial epithelium, and some punctate fluorescence was observed in pneumocytes colocalized with pro-surfactant-associated protein C (SFTPC) as alveolar epithelial type II cell marker **(Fig. 1B)**. These results indicate that ET-2 is expressed in some bronchial epithelial cells and some alveolar epithelial type II cells.

We next genetically inactivated *ET-2* expression in the epithelium by generating ET-$2^{flox/flox}$; SHH-$Cre^{+/-}$ mice. These mice were born without any apparent abnormalities and grew normally into adulthood. *ET-2* mRNA expression was markedly downregulated in the lungs and small intestines of ET-$2^{flox/flox}$; SHH-$Cre^{+/-}$ mice. Unexpectedly, *ET-1* mRNA levels demonstrated a decreasing tendency in the lungs **(Fig. 1C)**. ET-$2^{flox/flox}$; SHH-$Cre^{+/-}$ mice showed no apparent difference in body weight and food consumption compared to ET-$2^{flox/flox}$ littermates **(Fig. 1D)**. Parameters of pulmonary mechanics, lung histology, and collagen deposition showed no apparent differences between ET-$2^{flox/flox}$; SHH-$Cre^{+/-}$ and ET-$2^{flox/flox}$ mice **(Fig. 1E-F)**. Collectively, these results indicate that despite being primarily expressed in epithelial cells, epithelial ET-2 is not essential for growth and normal lung development.

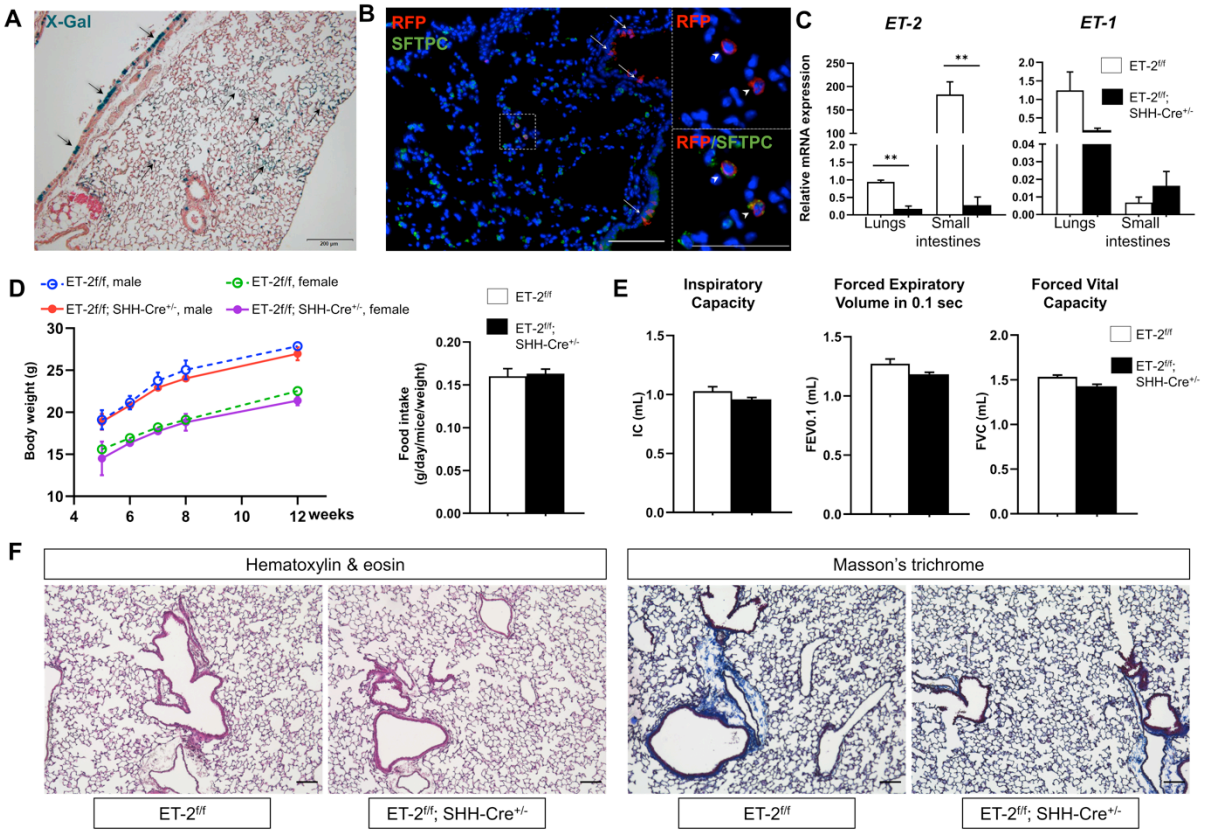

Figure 1. Endothelin (ET)-2 is expressed in the epithelial cells of mouse lungs. (A) X-Gal staining in the lung tissue of ET-2-iCre; ROSA26-lacZ mice. Black arrows indicate ET-2 stained with X-Gal (blue). Scale bar, 200 µm. (B) Red fluorescence protein (RFP) and pro-surfactant-associated protein C (SFTPC) staining in the lungs of ET-2-iCre; Ai9 mice. White arrows indicate RFP expression in the bronchiolar epithelium. White box indicates colocalization of RFP and SFTPC in pneumocytes, pointed by white arrowheads. Scale bars, 50 µm. (C) *ET-2* and *ET-1* relative mRNA expression in the lungs or small intestines of ET-$2^{flox/flox}$ (ET-$2^{f/f}$) and ET-$2^{flox/flox}$; SHH-$Cre^{+/-}$ (ET-$2^{f/f}$; SHH-$Cre^{+/-}$) mice (n = 3 each). **P < 0.01. (D) Body weight and food intake of ET-$2^{f/f}$ and ET-$2^{f/f}$; SHH-$Cre^{+/-}$ mice (n = 4 each). (E) Analysis of the lung mechanics of ET-$2^{f/f}$ and ET-$2^{f/f}$; SHH-$Cre^{+/-}$ mice (n = 2 each). (F) H-E and Masson's trichrome staining of the lungs of ET-$2^{f/f}$ and ET-$2^{f/f}$; SHH-$Cre^{+/-}$ mice. Scale bars, 100µm.

Exacerbation of lung fibrosis in ET-2$^{flox/flox}$; SHH-Cre$^{+/-}$ mice following bleomycin administration

We further studied the role of ET-2 in pulmonary fibrosis using bleomycin-induced pulmonary fibrosis mice model. After bleomycin treatment, *ET-1, ET_A*, and *ET_B* mRNA levels were upregulated in the control mouse lung tissue, whereas *ET-2* mRNA levels were downregulated **(Fig. 2A)**. Next, we subjected ET-2$^{flox/flox}$; SHH-Cre$^{+/-}$ and ET-2$^{flox/flox}$ mice to bleomycin intratracheal instillation. Notably, ET-2$^{flox/flox}$; SHH-Cre$^{+/-}$ mice exhibited higher collagen deposition after bleomycin treatment than ET-2$^{flox/flox}$ littermates **(Fig. 2B-C)**. Consistent with this result, pulmonary mechanics analyzed after 21 days following bleomycin administration showed increased tissue damping and suppressed static compliance in ET-2$^{flox/flox}$; SHH-Cre$^{+/-}$ mice compared to ET-2$^{flox/flox}$ mice **(Fig. 2D)**.

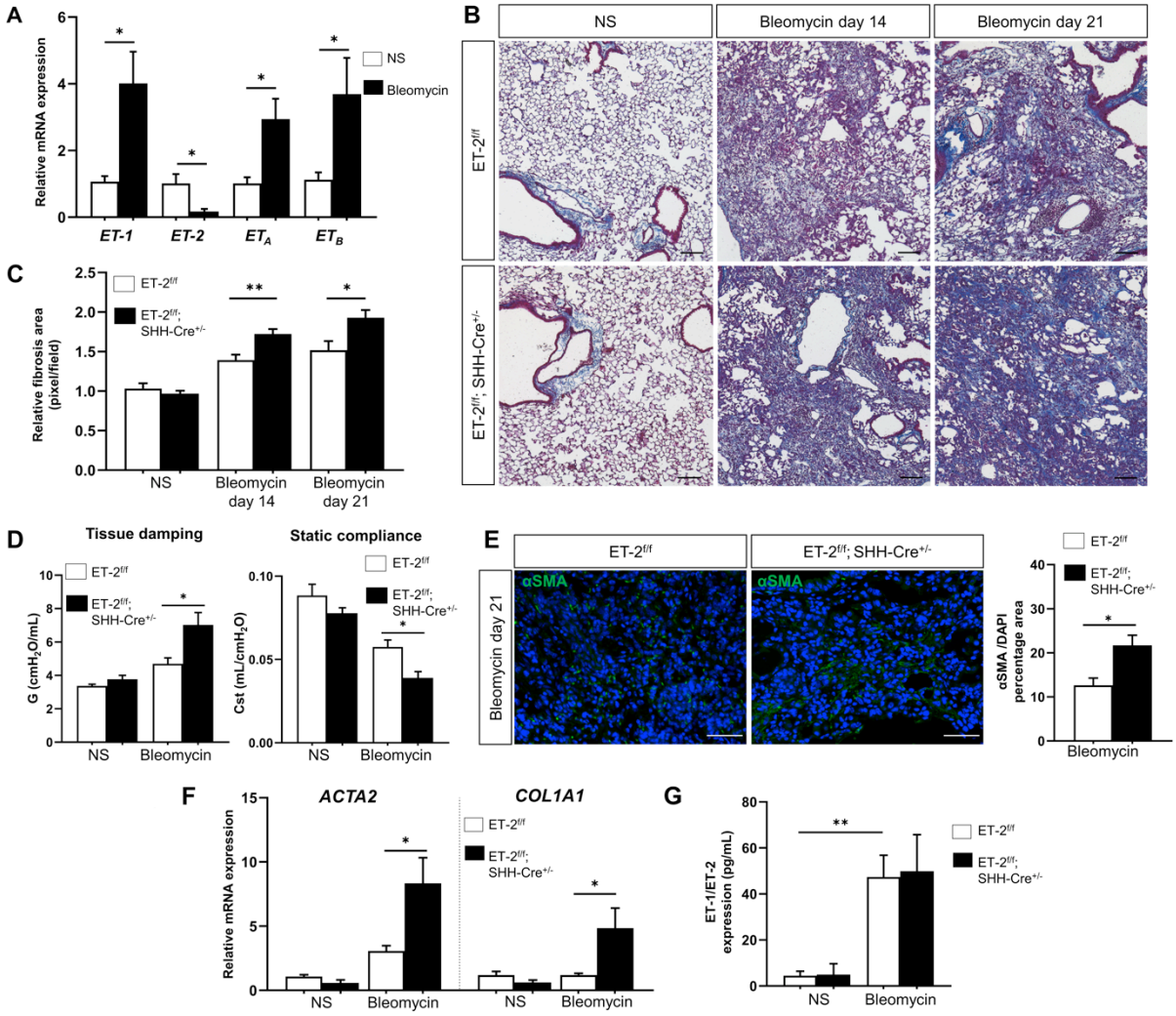

Figure 2. Deletion of endothelin (ET)-2 in the epithelial cells exacerbates bleomycin-induced pulmonary fibrosis in mice. (A) *ET-1, ET-2, ET_A,* and *ET_B* mRNA expression observed in the lung tissues after normal saline (NS) or bleomycin administration for 28 days (n = 4-5 each). *P < 0.1. (B) Representative images of lung Masson's trichrome staining in the lungs of ET-2$^{flox/flox}$ (ET-2$^{f/f}$) and ET-2$^{flox/flox}$; SHH-Cre$^{+/-}$ (ET-2$^{f/f}$; SHH-Cre$^{+/-}$) mice following the administration of N.S. or bleomycin for the indicated days (n=3 each for NS, 5–6 each for bleomycin-treated groups). Scale bars, 100 μm. (C) Quantification of relative fibrosis area percentage of Fig. 2B (n=3 each for NS, 5–6 each for bleomycin-treated groups). The result was normalized to NS ET-2$^{f/f}$ group. *P < 0.05, **P < 0.01. (D) Tissue damping and static compliance of the lungs of ET-2$^{f/f}$ and ET-2$^{f/f}$; SHH-Cre$^{+/-}$ mice after intratracheal administration of N.S. or bleomycin for 21 days (n = 3 each for NS, 5 each for bleomycin-treated group). *P < 0.05. (E) Representative image and quantification of αSMA / DAPI positive area in the lungs of ET-2$^{f/f}$ and ET-2$^{f/f}$; SHH-Cre$^{+/-}$ mice after bleomycin instillation for 21 days (n = 5–6). Scale bars, 50 μm. *P < 0.05. (F) Relative mRNA expression of *ACTA2* and *COL1A1* in the lungs of ET-2$^{f/f}$ and ET-2$^{f/f}$; SHH-Cre$^{+/-}$ mice after N.S. or bleomycin administration for 21 days. (n = 3 each for NS, 6 each for bleomycin-treated groups). *P < 0.05. (G) ET-1/ET-2 concentration in the lungs of ET-2$^{f/f}$ and ET-2$^{f/f}$; SHH-Cre$^{+/-}$ mice measured after NS or bleomycin administration for 21 days (n = 2–3 for NS, 4–7 for bleomycin groups) **P < 0.01.

Furthermore, the lung tissue of ET-2$^{flox/flox}$; SHH-Cre$^{+/-}$ mice demonstrated abundant expression of myofibroblast marker (alpha-smooth muscle actin; αSMA) after bleomycin treatment compared to that of ET-2$^{flox/flox}$ mice, indicating an increase in myofibroblast infiltration in the lungs of ET-2$^{flox/flox}$; SHH-Cre$^{+/-}$ mice **(Fig. 2E)**. Moreover, the mRNA expression levels of fibroblast activation marker, *ACTA2* and extracellular matrix (ECM) collagen marker, *COL1A1* were increased in the lung tissues of ET-2$^{flox/flox}$; SHH-Cre$^{+/-}$ mice **(Fig. 2F)**. We next measured ET-1/ET-2 expression in the mouse lungs using ELISA ET-1 immunoassay, which exhibited 51% cross-reactivity with ET-2 peptide. Although bleomycin administration significantly increased the expression of ET-1/ET-2 in the lungs, no difference in ET-1/ET-2 expression was observed between ET-2$^{flox/flox}$; SHH-Cre$^{+/-}$ and ET-2$^{flox/flox}$ mice **(Fig. 2G)**. Hence, the detrimental conditions of the lungs found in ET-2$^{flox/flox}$; SHH-Cre$^{+/-}$ mice could not be attributed to an increase in ET-1 expression. These results indicate that deletion of ET-2 in epithelial cells exacerbates bleomycin-induced lung fibrosis in mice.

Silencing of ET-2 enhances apoptosis and oxidative stress in A549 epithelial cells

To further investigate the differences between the roles of ET-1 and ET-2 in pulmonary fibrosis pathophysiology, we used A549 cell line as a suitable model of type II alveolar epithelial cells (24). Successful silencing of *ET-1* or *ET-2* was confirmed by examining the corresponding mRNA expression and secreted ET-1/ET-2 from these cells **(Fig. 3A-B)**. We next exposed cells with *ET-1* or *ET-2* knockdown to hydrogen peroxide (H_2O_2)-induced oxidative stress (25). Notably, cells with *ET-2*, but not *ET-1,* knockdown, exhibited an increase in cleaved-caspase-3 levels, also cleaved-caspase-8 and 9, that act as extrinsic and intrinsic apoptosis markers following H_2O_2 stimulation **(Fig. 3C)**. Collectively, these results suggest that ET-2 depletion enhanced apoptosis in A549 cells, probably by upregulating extrinsic and intrinsic apoptosis pathways.

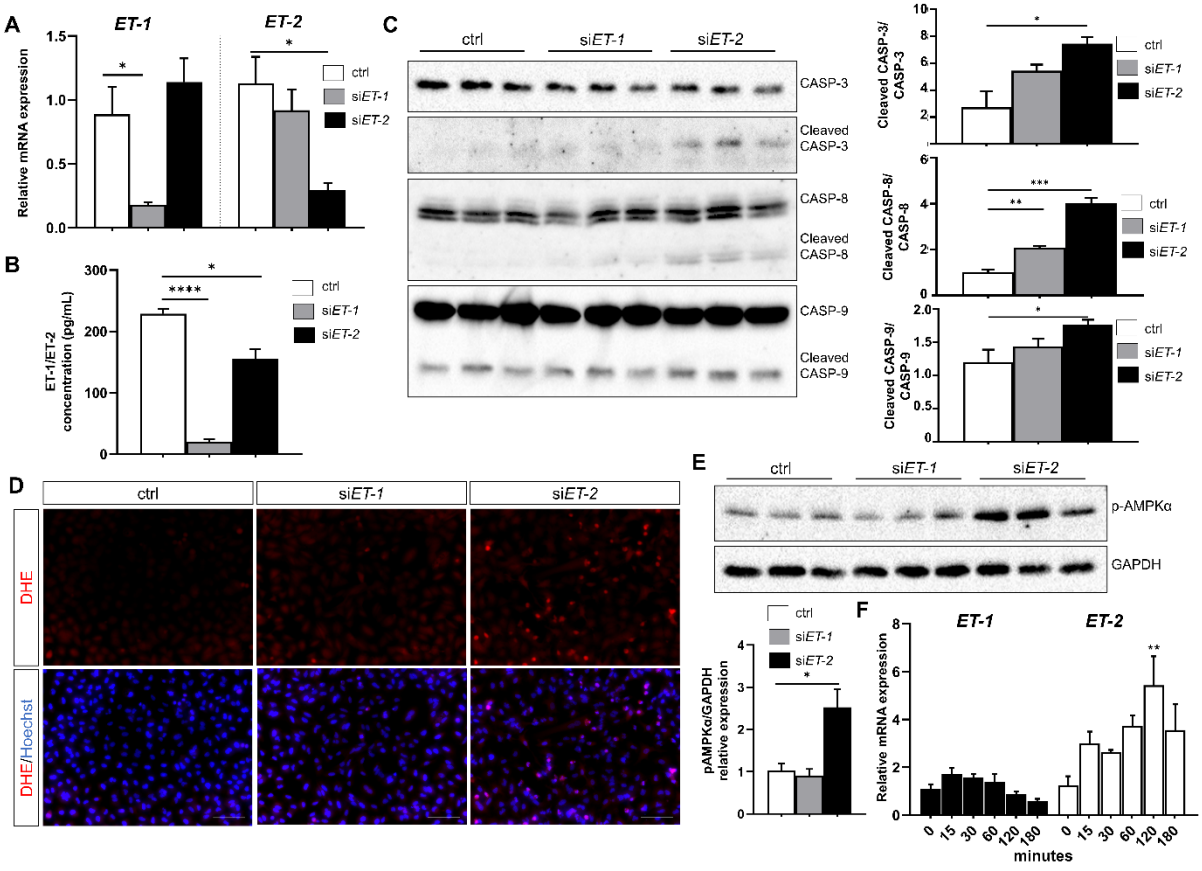

Figure 3. Endothelin (*ET)-2* knockdown increases apoptosis in A549 cells. (A) Relative mRNA expression of *ET-1* and *ET-2* in control and A549 cells with *ET-1* or *ET-2* knockdown (n = 3 each). *P < 0.05. (B) Concentration of ET-1/ET-2 in the medium collected from the control and A549 cells with *ET-1* or *ET-2* knockdown (n = 3 each). *P < 0.05, ****P < 0.0001. (C) Immunoblotting for apoptosis protein markers, ratio of Cleaved Caspase (CASP)-3/CASP-3, Cleaved CASP-8/CASP-8, and Cleaved CASP-9/CASP-9 in control and A549 cells with *ET-1* or *ET-2* knockdown (n = 3 each) after treatment with H_2O_2. *P < 0.05; **P < 0.01; ***P < 0.001. (D) Representative image of dihydroethidium (DHE) staining of the control and A549 cells with *ET-1* or *ET-2* knockdown. Scale bars, 100 µm. (E) Immunoblotting for phospho-AMPKα (pAMPKα) protein expression in control and A549 cells with *ET-1* or *ET-2* knockdown (n = 3 each) after treatment with H_2O_2. *P < 0.05. (F) Relative mRNA expression levels of *ET-1* and *ET-2* after stimulation of A549 cells with H_2O_2 for indicated duration (n = 3 each). **P < 0.01 assessed by one-way ANOVA.

Furthermore, knockdown of *ET-2*, but not *ET-1*, caused excessive superoxide production judged by dihydroethidium staining in A549 cells **(Fig. 3D)**, and enhanced phospho-AMPKα expression in H_2O_2-treated A549 cells **(Fig. 3E)**. In addition, *ET-2* mRNA expression, but not *ET-1*, was upregulated in A549 cells after H_2O_2 stimulation **(Fig. 3F)**. These results suggest that ET-2 expression is upregulated after induction of oxidative stress, and silencing *ET-2* in A549 cells enhances oxidative stress.

Exogenous ET-2 inhibits fibroblast migration and hampers TGF-β-induced fibroblast activation

We further explored the roles of ET-2 and ET-1 in mouse lung fibroblasts. Our results showed that the migration of mouse lung fibroblasts was increased after incubation with recombinant ET-1, confirming the ability of ET-1 to promote fibroblast migration (26). In contrast, a reduction in migration was observed in recombinant ET-2–treated cells, suggesting that ET-2 suppresses fibroblast invasiveness **(Fig. 4A)**.

We next examined exogenous endothelin effects upon TGF-β-induced fibroblast activation. Notably, the expression of *ACTA2* and *COL1A1* markers was increased in the ET-1-treated group, but decreased in the ET-2-treated group after TGF-β induction **(Fig. 4B)**. Consistently, TGF-β-induced SMAD2/3 activation was increased in the ET-1-treated group, but decreased in the ET-2-treated group **(Fig. 4C)**. These results collectively indicate that in contrast to ET-1, ET-2 blocks mouse lung fibroblast activation and extracellular matrix production via inhibition of TGF-β–SMAD2/3 signaling.

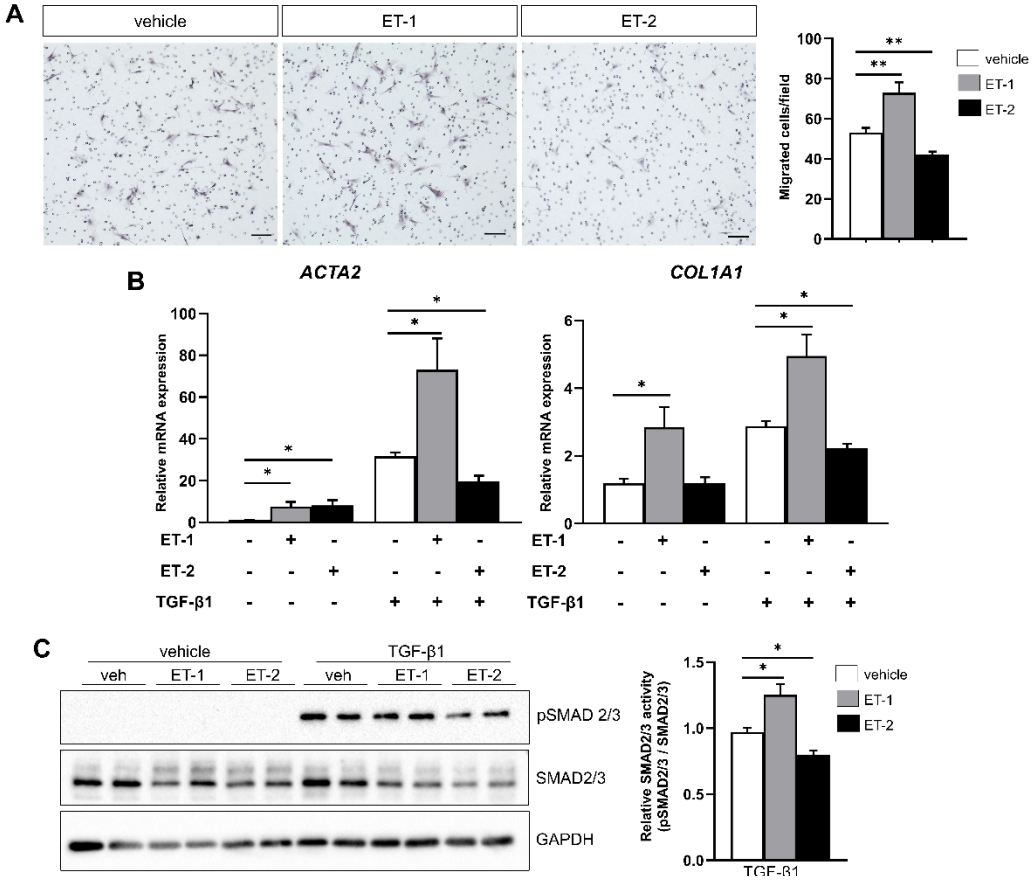

Figure 4. Endothelin (ET)-2 inhibits transforming growth factor (TGF)-β induced mouse lung fibroblast activation. (A) Representative image showing the results of migration assay for the vehicle, recombinant ET-1, or ET-2 treated groups (n = 7 each group). Scale bars, 100 μm. **P < 0.01. (B) Relative mRNA expression of *ACTA2* and *COL1A1* after TGF-β1 stimulation for 24 h in the vehicle, recombinant ET-1, or ET-2 treated groups (n = 4 each group). *P < 0.05. (C) Immunoblotting for phospho-SMAD2/3 (pSMAD2/3) and SMAD2/3 protein expression levels in the vehicle and recombinant ET-1 or ET-2 treated groups after stimulation with TGF-β1 for 1 h and relative quantification of SMAD2/3 activity (n = 3 each group). *P < 0.05.

DISCUSSION

In the present study, we demonstrated that ET-2 is mainly expressed in epithelial cells in the mouse lungs. Epithelial ET-2 exerts a protective effect against bleomycin-induced pulmonary fibrosis in mice, probably by inhibiting epithelial apoptosis. In mouse lung fibroblasts, ET-2 and ET-1 exert opposite effects on fibroblast migration and activation.

Our results confirmed that ET-2 is expressed in the epithelial cells of the lungs (12). Notably, specific deletion of ET-2 in epithelial cells resulted in normal lung development. This phenotype was different from that observed upon global knockout in neonatal mice, demonstrating abnormalities in the lung development, and from that observed upon conditional global knockout in adult mice, resulting in the structural and functional abnormalities of the lungs (13). Hence, epithelial ET-2 is unlikely to be involved in early lung development, suggesting that ET-2 secreted from other cells might play a more significant role in this process.

In contrast to ET-2 that expressed in the lung epithelium, ET-1, ET_A and ET_B are expressed mostly in lung mesenchyme (13,27). Bleomycin treatment will change lung cell population as epithelial cells are damaged and decreased, while mesenchymal cells are increased (28). Increase expression of ET-1, ET_A, and ET_B in mesenchyme after bleomycin treatment was also explained previously (27,29). Thus, the decrease of *ET-2* expression after bleomycin treatment potentially arises from the alteration of lung cell population.

Lung fibrosis is characterized by alterations in the epithelial cells, such as epithelial-to-mesenchymal transition, apoptosis, and senescence (30). Apoptosis in alveolar epithelial type II cells was observed in patients with lung fibrosis as an initial response to epithelial damage (30,31), mainly induced by oxidative stress (32). Our results implied that ET-2 in epithelial cells plays a role in inhibiting apoptosis. Silencing *ET-2* in A549 epithelial cells enhanced apoptosis due to excessive superoxide production, and a transient increase in ET-2 expression was observed after oxidative stress induction. These results raise the possibility that the induction of oxidative stress may transiently induce ET-2 expression to further protect the cells from apoptosis.

An increase in fibroblast infiltration via the basement membrane, myofibroblast differentiation, and ECM collagen deposition characterizes maladaptive repair in lung fibrosis and acts as critical factors of pulmonary fibrosis progression (30). These mechanisms are widely known to be regulated by TGF-β by activating its canonical SMAD-dependent signaling of fibroblast activation and ECM protein synthesis (30,33). ET-1 is upregulated during tissue repair and promotes myofibroblast contraction, contributing to matrix remodeling during tissue repair (26). Interestingly, our result showed that ET-$2^{flox/flox}$; SHH-$Cre^{+/-}$ treated with bleomycin increased myofibroblast accumulation, raising the possibility of whether ET-2 exerts a different role from ET-1 in lung fibroblast activation. In the present study, we confirmed that ET-1 increased migration and activation of lung fibroblasts following TGF-β-induced fibroblast activation and collagen synthesis. In contrast, ET-2 suppressed the invasion and activation of mouse lung fibroblasts, potentially via inhibition of SMAD2/3 phosphorylation, suggesting that the balance of ET-1 and ET-2 may contribute to the development of pulmonary fibrosis.

ET-1 expression increased in bleomycin-induced lung fibrosis in mice, and bosentan, a dual ERA, attenuated collagen deposition in the same animal model (16). Since then, ERAs have been proposed as a promising treatment for interstitial lung disease, and several clinical trials have been conducted to evaluate the effects of the ERA regimen for this disease. However, ERA clinical trials using macitentan and bosentan did not demonstrate any differences in the outcomes compared to those observed with placebo (17,18). Furthermore, clinical trials examining the effect of ambrisentan, a specific ET_A antagonist, demonstrated worsening of patient conditions as disease progression aggravated, and the death rate increased compared to those observed with placebo (19). These distinctive effects in mouse models and human studies have implied the possibility of another peptide acting through the same receptors as ET-1 but exerting different effects in the lungs.

It has been known that GPCR showed biased signaling upon certain ligands stimulation. Certain ligands stabilize distinct receptor conformation and preferentially activating the canonical G protein signaling pathway or non-G protein transducers, including β-arrestin, leading to different signals transduction (34). Therefore, although ET-1 and ET-2 shared similar affinity to ET_A and ET_B receptors, we speculate that signal transduction triggered by ET-1 and ET-2 ligands might be different. Therefore, it is important to consider the distinct molecular pathway induced by ET-1 and ET-2 despite their structural and pharmacological similarities. In the future, further studies would be necessary to elucidate the distinct cascades in order to design a novel treatment strategy targeting endothelin receptor-specific signal transduction pathways to combat uncured target diseases, including pulmonary fibrosis.

ABBREVIATIONS

ET, endothelin; ERAs, endothelin receptor antagonists; TGF, transforming growth factor; ET_A, endothelin A; ET_B, endothelin B; iCre, codon-improved Cre recombinase; RFP, red fluorescence protein; SFTPC, pro-surfactant-associated protein C; αSMA, alpha-smooth muscle actin; ECM, extracellular matrix; H_2O_2, hydrogen peroxide; NS, normal saline

FUNDING

This study was supported by JSPS KAKENHI (Grant Number JP19H03382 to N.E.).

ACKNOWLEDGEMENTS

We thank Ratih Paramita Suprapto, Gusty Rizky Teguh Ryanto, and Ahmad Musthafa for their valuable discussions.

CONFLICT OF INTEREST

The authors declare no conflict of interest.

REFERENCES

1. **Davenport, A.P., Hyndman, K.A., Dhaun, N., Southan, C., Kohan, D.E., Pollock, J.S., Pollock, D.M., Webb, D.J., and Maguire, J.J.** 2016. Endothelin. Pharmacol Rev **68**: 357–418.
2. **Maguire, J.J. and Davenport, A.P.** 1995. ET_A receptor-mediated constrictor responses to endothelin peptides in human blood vessels in vitro. Br J Pharmacol **115**: 191–7.
3. **Saida, K., Mitsui, Y., and Ishida, N.** 1989. A novel peptide, vasoactive intestinal contractor, of a new (endothelin) peptide family. J Biol Chem **264**: 14613–6.
4. **Ling, L., Maguire, J.J., and Davenport, A.P.** 2013. Endothelin-2, the forgotten isoform: Emerging role in the cardiovascular system, ovarian development, immunology and cancer. Br J Pharmacol **168**: 283–95.
5. **Ko, C., Gieske, M.C., Al-Alem, L., Hahn, Y.K., Su, W., Gong, M.C., Iglarz, M., and Koo, Y.** 2006. Endothelin-2 in ovarian follicle rupture. Endocrinology **147**: 1770–9.
6. **Rattner, A., Yu, H., Williams, J., Smallwood, P.M., and Nathans, J.** 2013. Endothelin-2 signaling in the neural retina promotes the endothelial tip cell state and inhibits angiogenesis. Proc Natl Acad Sci **110**: E3830–9.
7. **Grimshaw, M.J., Wilson, J.L., and Balkwill, F.R.** 2002. Endothelin-2 is a macrophage chemoattractant: Implications for macrophage distribution in tumors. Eur J Immunol **32**: 2393–400.
8. **Takizawa, S., Uchide, T., Adur, J., Kozakai, T., Kotake-Nara, E., Quan, J., and Saida, K.** 2005. Differential expression of endothelin-2 along the mouse intestinal tract. J Mol Endocrinol **35**: 201–9.
9. **Kakinuma, Y., Miyauchi, T., Kobayashi, T., Yuki, K., Maeda, S., Sakai, S., Goto, K., and Yamaguchi, I.** 1999. Myocardial expression of endothelin-2 is altered reciprocally to that of endothelin-1 during ischemia of cardiomyocytes in vitro and during heart failure in vivo. Life Sci **65**: 1671–83.
10. **Grimshaw, M.J., Naylor, S., and Balkwill, F.R.** 2002. Endothelin-2 is a hypoxia-induced autocrine survival factor for breast tumor cells. Mol Cancer Ther **1**: 1273–81.
11. **Tanese, K., Fukuma, M., Ishiko, A., and Sakamoto, M.** 2010. Endothelin-2 is upregulated in basal cell carcinoma under control of Hedgehog signaling pathway. Biochem Biophys Res Commun **391**: 486–91.
12. **Cacioppo, J., Koo, Y., Lin, P.C.P., Gal, A., and Ko, C.** 2015. Generation and characterization of an Endothelin-2 iCre mouse. Genesis. **53**: 48–55.
13. **Chang, I., Bramall, A.N., Baynash, A.G., Rattner, A., Rakheja, D., Post, M., Joza, S., McKerlie, C., Stewart, D.J., McInnes, R.R., and Yanagisawa, M.** 2013. Endothelin-2 deficiency causes growth retardation, hypothermia, and emphysema in mice. J Clin Invest **123**: 2643–53.
14. **Saleh, D., Furukawa, K., Tsao, M.S., Maghazachi, A., Corrin, B., Yanagisawa, M., Barnes, P.J., and Giaid, A.** 1997. Elevated expression of endothelin-1 and endothelin-converting enzyme-1 in idiopathic pulmonary fibrosis: possible involvement of proinflammatory cytokines. Am J Respir Cell Mol Biol **16**: 187–93.
15. **Hocher, B., Schwarz, A., Fagan, K.A., Thöne-Reineke, C., El-Hag, K., Kusserow, H, Elitok, S., Bauer, C., Neumayer, H, Rodman, D.M., and Theuring, F.** 2000. Pulmonary fibrosis and chronic lung inflammation in ET-1 transgenic mice. Am J Respir Cell Mol Biol **23**: 19–26.
16. **Park, S.H, Saleh, D., Giaid, A., and Michel, R.P.** 1997. Increased endothelin-1 in bleomycin-induced pulmonary fibrosis and the effect of an endothelin receptor antagonist. Am J Respir Crit Care Med **156**: 600-8.
17. **King, T.E., Brown, K.K., Raghu, G., du Bois, R.M., Lynch, D.A., Martinez, F., Valeyre, D., Leconte, I., Morganti, A., Roux, S., and Behr, J.** 2011. BUILD-3: A randomized, controlled trial of bosentan in idiopathic pulmonary fibrosis. Am J Respir Crit Care Med **184**: 92–9.
18. **Raghu, G., Million-Rousseau, R., Morganti, A., Perchenet, L., Behr, J., and MUSIC Study Group.** 2013. Macitentan for the treatment of idiopathic pulmonary fibrosis: The randomised controlled MUSIC trial. Eur Respir J **42**: 1622–32.
19. **Raghu, G., Behr, J., Brown, K.K., Egan, J.J., Kawut, S.M., Flaherty, K.R., Martinez, F.J., Nathan, S.D., Wells, A.U., Collard, H.R., Costabel, U., Richeldi, L., de Andrade, J., Khalil, N., Morrison, L.D., Lederer, D.J., Shao, L., Li, X., Pedersen, P.S., Montgomery, A.B., Chien, J.W., O'Riordan, T.G., and ARTEMIS-IPF Investigators.** 2013. Treatment of idiopathic pulmonary fibrosis with ambrisentan: a

parallel, randomized trial. Ann Intern Med **158**: 641-9.
20. **Harfe, B.D., Scherz, P.J., Nissim, S., Tian, H., McMahon, A.P., and Tabin, C.J.** 2004. Evidence for an expansion-based temporal Shh gradient in specifying vertebrate digit identities. Cell **118**: 517–28.
21. **Rahardini, E.P., Ikeda, K., Nugroho, D.B., Hirata, K., and Emoto, N.** 2019. Loss of family with sequence similarity 13, member A exacerbates pulmonary fibrosis potentially by promoting epithelial to mesenchymal transition. Kobe J Med Sci **65**: E100–9.
22. **Hartopo, A.B., Emoto, N., Vignon-Zellweger, N., Suzuki, Y., Yagi, K., Nakayama, K., and Hirata, K.** 2013. Endothelin-converting enzyme-1 gene ablation attenuates pulmonary fibrosis via CGRP-cAMP/EPAC1 pathway. Am J Respir Cell Mol Biol. **48**: 465–76.
23. **Lovgren, A.K., Kovacs, J.J., Xie, T., Potts, E.N., Li, Y., Foster, W.M., Liang, J., Meltzer, E.B., Jiang, D., Lefkowitz, R.J., and Noble, P.W.** 2011. β-arrestin deficiency protects against pulmonary fibrosis in mice and prevents fibroblast invasion of extracellular matrix. Sci Transl Med **3**: 74ra23.
24. **Foster, K.A., Oster, C.G., Mayer, M.M., Avery, M.L., and Audus, K.L.** 1988. Characterization of the A549 cell line as a type II pulmonary epithelial cell model for drug metabolism. Exp Cell Res **243**: 359–66.
25. **Zmijewski, J.W., Banerjee, S., Bae, H., Friggeri, A., Lazarowski, E.R., and Abraham, E.** 2010. Exposure to hydrogen peroxide induces oxidation and activation of AMP-activated protein kinase. J Biol Chem **285**: 33154–64.
26. **Shi-Wen, X., Chen, Y., Denton, C.P., Eastwood, M., Renzoni, E.A., Bou-Gharios, G., Pearson, J.D., Dashwood, M., du Bois, R.M., Black, C.M., Leask, A., and Abraham, D.J.** 2004. Endothelin-1 promotes myofibroblast induction through the ETA receptor via a rac/phosphoinositide 3-kinase/Akt-dependent pathway and is essential for the enhanced contractile phenotype of fibrotic fibroblasts. Mol Biol Cell **15**: 2707–19.
27. **Swigris, J.J. and Brown, K.K.** 2010. The role of endothelin-1 in the pathogenesis of idiopathic pulmonary fibrosis. Biodrugs. **24**: 49–54.
28. **Dorry, S.J., Ansbro, B.O., Ornitz, D.M., Mutlu, G.M., and Guzy, R.D.** 2020. FGFR2 is required for AEC2 homeostasis and survival after bleomycin-induced lung injury. Am J Respir Cell Mol Biol **62**: 608–21.
29. **Wendel, M., Petzold, A., Koslowski, R., Kasper, M., Augstein, A., Knels, L., Bleyl, J.U., and Koch, T.** 2000. Localization of endothelin receptors in bleomycin-induced pulmonary fibrosis in the rat. Histochem Cell Biol **122**: 507–17.
30. **Martinez, F.J., Collard, H.R., Pardo, A., Raghu, G., Richeldi, L., Selman, M., Swigris, J.J., Taniguchi, H., and Wells, A.U.** 2017. Idiopathic pulmonary fibrosis. Nat Rev Dis Prim. **3**: 1–20.
31. **Uhal, B.D.** 2008. The role of apoptosis in pulmonary fibrosis. Eur Respir Rev **17**: 138–44.
32. **Cheresh, P., Kim, S.J., Tulasiram, S., and Kamp, D.W.** 2013 Oxidative stress and pulmonary fibrosis. Biochim Biophys Acta - Mol Basis Dis **1832**: 1028–40.
33. **Frangogiannis, N.G.** 2020. Transforming growth factor–ß in tissue fibrosis. J Exp Med **217**: 1–16.
34. **Smith, J.S., Lefkowitz, R.J., and Rajagopal, S.** 2018. Biased signalling: From simple switches to allosteric microprocessors. Nat Rev Drug Discov. **17**: 243-60.

Table I. Nucleotide sequence for quantitative PCR primers

Primer	Forward	Reverse
Mouse *ET-2*	TCTGCCACCTGGACATCATC	GAGCACTCACAACGCTTTGG
Mouse *ET-1*	TGTATCTATCAGCAGCTGGTGGAA	AAAAATGCCTTGATGCTATTGC
Mouse ET_A	TATCCTGCACCATTTTCATCGTGGG	ATAAGGTCTCCAAGGGCCAGGCT
Mouse ET_B	CATGCGCAATGGTCCCAATA	GCTCCAAATGGCCAGTCCTC
Mouse *ACTA2*	ACAGAGGCACCACTGAACCCTAAG	ACAATCTCACGCTCGGCAGTAGTC
Mouse *COL1A1*	CCGTGCTTCTCAGAACATCA	AGCATCCATCTTGCAGCCTTG
Mouse *GAPDH*	TGTGTCCGTCGTGGATCTGA	TTGCTGTTGAAGTCGCAGGAG
Human *ET-2*	CTTCTCCAAAGGCTGAGGGACATT	TCCTGTTGTCGCTTGGCAAAGA
Human *ET-1*	TTCTCTCTGCTGTTTGTGGCTTGC	TCTTTATCCATCAGGGACGAGCAG
Human/mouse *18S*	GTAACCCGTTGAACCCCATT	CCATCCAATCGGTAGTAGCG